

Inhibition of a type III secretion system by the deletion of a short loop in one of its membrane proteins

Vladimir A. Meshcheryakov,^a
Akio Kitao,^{b,c} Hideyuki
Matsunami^a and Fadel A.
Samatey^{a*}

^aTrans-Membrane Trafficking Unit,
Okinawa Institute of Science and Technology,
Okinawa 904-0495, Japan, ^bInstitute of
Molecular and Cellular Biosciences, University
of Tokyo, Tokyo 113-0032, Japan, and
^cJapan Science and Technology Agency,
Core Research for Evolutionary Science and
Technology, Tokyo 113-0032, Japan

Correspondence e-mail: f.a.samatey@oist.jp

The membrane protein FlhB is a highly conserved component of the flagellar secretion system. It is composed of an N-terminal transmembrane domain and a C-terminal cytoplasmic domain (FlhB_C). Here, the crystal structures of FlhB_C from *Salmonella typhimurium* and *Aquifex aeolicus* are described at 2.45 and 2.55 Å resolution, respectively. These flagellar FlhB_C structures are similar to those of paralogues from the needle type III secretion system, with the major difference being in a linker that connects the transmembrane and cytoplasmic domains of FlhB. It was found that deletion of a short flexible loop in a globular part of *Salmonella* FlhB_C leads to complete inhibition of secretion by the flagellar secretion system. Molecular-dynamics calculations demonstrate that the linker region is the most flexible part of FlhB_C and that the deletion of the loop reduces this flexibility. These results are in good agreement with previous studies showing the importance of the linker in the function of FlhB and provide new insight into the relationship between the different parts of the FlhB_C molecule.

Received 31 October 2012

Accepted 21 January 2013

PDB References: *Salmonella*
FlhB_C, 3b0z; *Aquifex* FlhB_C,
3b1s

1. Introduction

The bacterial flagellum is a large complex structure that is used as a motility organelle by many bacteria. It consists of three main substructures: the basal body, the hook and the filament. Most of the flagellar proteins are localized outside the cell and are translocated across the cell membrane by the flagellum-specific secretion apparatus, which is evolutionarily and structurally related to the virulence type III secretion system (Aizawa, 2001; Blocker *et al.*, 2003). Protein export by the flagellar type III secretion system is highly regulated. The secretion system first exports rod/hook-type proteins until the hook reaches an appropriate length. The secretion system then switches substrate specificity from hook-type export to filament-type export (Minamino & Macnab, 1999; Hirano *et al.*, 2003). In *Salmonella*, the substrate-specificity switch is controlled by two proteins: FliK and FlhB (Kutsukake *et al.*, 1994; Hirano *et al.*, 1994; Williams *et al.*, 1996).

FlhB is an essential membrane protein of the flagellar type III secretion system. It consists of two domains: a hydrophobic N-terminal part (FlhB_{TM}) that is predicted to contain four transmembrane helices and a C-terminal cytoplasmic domain (FlhB_C) (Minamino *et al.*, 1994). The two domains are connected by a flexible linker. This linker is a highly conserved part of the FlhB protein and is essential for the type III secretion system (TTSS). Deletions or point mutations in the linker region completely abolish or significantly reduce secretion (Fraser *et al.*, 2003; Zarivach *et al.*, 2008). The wild-type cytoplasmic domain of *Salmonella* FlhB undergoes autocatalytic cleavage between amino-acid residues Asn269

and Pro270 within a highly conserved NPTH sequence (Minamino & Macnab, 2000a). This autocleavage is essential for the switching process (Fraser *et al.*, 2003; Ferris *et al.*, 2005). Mutation of Asn269 to Ala prevents cleavage and locks the export apparatus in the hook-type specificity state.

FlhB_C has been shown to interact with several soluble components of the TTSS: FliH, FliI, FliJ (Minamino & Macnab, 2000b), the cytoplasmic part of the membrane protein FlhA (Zhu *et al.*, 2002) and the hook-length control protein FliK (Minamino *et al.*, 2004; Morris *et al.*, 2010). Interaction of FlhB with FliK has been suggested to be important for the substrate-specificity switching process (Ferris & Minamino, 2006). Cells with a deleted *fliK* gene produce an abnormally long hook, termed a 'polyhook', without any filament attached (Hirano *et al.*, 1994).

Several structures of the cytoplasmic domain of FlhB paralogues from the needle TTSS have been published (Zarivach *et al.*, 2008; Deane *et al.*, 2008; Wiesand *et al.*, 2009; Lountos *et al.*, 2009). However, no structural information is available for FlhB from the flagellar secretion system. Here, we describe crystal structures of the cytoplasmic domain of flagellar FlhB from two organisms: *Salmonella typhimurium* and *Aquifex aeolicus*.

2. Materials and methods

2.1. Structure determination

Details of the purification, crystallization and data collection of *Salmonella* and *Aquifex* FlhB_C have been described previously (Meshcheryakov *et al.*, 2011; Meshcheryakov & Samatey, 2011). Both structures were solved by multi-wavelength anomalous diffraction (MAD) using the program *SHELXD* (Sheldrick, 2008). Initial protein models were built automatically with *Buccaneer* (Cowtan, 2006) from the *CCP4* package (Winn *et al.*, 2011). The models were refined through an iterative combination of refinement with *REFMAC5* (Murshudov *et al.*, 2011) and manual model building in *Coot* (Emsley *et al.*, 2010). In the case of *Salmonella* FlhB_C, TLS refinement was performed in the final stages with two TLS

Table 1

X-ray data-collection and refinement statistics.

Values in parentheses are for the highest resolution shell. MAD data-collection statistics for *Salmonella* FlhB_C have been published in Meshcheryakov & Samatey (2011).

	<i>Salmonella</i> FlhB _C		<i>Aquifex</i> FlhB _C		
	Native	Native	SeMet derivative		
			Peak	Inflection	Remote
Data collection					
Space group	<i>P4</i> ₂ <i>2</i> ₁ <i>2</i>	<i>C2</i>	<i>C2</i>		
Unit-cell parameters (Å, °)	<i>a</i> = <i>b</i> = 49.1, <i>c</i> = 143.1, $\alpha = \beta = \gamma = 90$	<i>a</i> = 114.6, <i>b</i> = 33.8, <i>c</i> = 122.4, $\alpha = \gamma = 90$, $\beta = 107.8$	<i>a</i> = 113.4, <i>b</i> = 33.6, <i>c</i> = 122.2, $\alpha = \gamma = 90$, $\beta = 107.9$		
Molecules in asymmetric unit	1	3	3		
Wavelength (Å)	0.9	0.9	0.9791	0.97936	0.99508
Resolution (Å)	40.45–2.45 (2.58–2.45)	47.76–2.55 (2.69–2.55)	50–3.00 (3.16–3.00)	50–3.00 (3.16–3.00)	50–3.00 (3.16–3.00)
<i>R</i> _{merge} [†] (<i>I</i> σ(<i>I</i>))	0.075 (0.380)	0.056 (0.386)	0.094 (0.452)	0.069 (0.407)	0.064 (0.368)
Completeness (%)	98.8 (100)	99.3 (100)	100 (100)	100 (100)	100 (100)
Multiplicity	7.7 (7.9)	3.7 (3.8)	3.6 (3.7)	3.7 (3.7)	3.7 (3.7)
Refinement					
Resolution (Å)	28.07–2.45	29.75–2.55			
<i>R</i> _{work} / <i>R</i> _{free} (%)	23.1/24.7	24.1/26.2			
No. of atoms					
Protein	992	2707			
Ligand/ion	4	0			
Water	20	48			
Wilson plot <i>B</i> factor (Å ²)	79.3	83.7			
Average <i>B</i> factor (Å ²)					
Protein	78.8	73.6			
Ligand/ion	77.2	N/A			
Water	39.3	61.2			
R.m.s. deviations					
Bond lengths (Å)	0.021	0.019			
Bond angles (°)	2.090	1.844			
Ramachandran plot (%)					
Most favoured	97.5	99.7			
Additionally allowed	2.5	0.3			
Disallowed	0	0			

[†] $R_{\text{merge}} = \sum_{hkl} \sum_i |I_i(hkl) - \langle I(hkl) \rangle| / \sum_{hkl} \sum_i I_i(hkl)$, where $I_i(hkl)$ is the intensity of the *i*th measurement of reflection *hkl* and $\langle I(hkl) \rangle$ is the mean value of $I_i(hkl)$ for all *i* measurements.

groups per FlhB_C molecule (residues 229–269 and 270–353; Painter & Merritt, 2006). Structural figures were produced using *PyMOL* (<http://www.pymol.org>).

2.2. DNA manipulation and motility assay

Mutations of *S. typhimurium flhB* carried by the plasmid pMM26 (Minamino & Macnab, 2000a) were performed as described previously (Wang & Malcolm, 1999). For the motility assay, freshly transformed *Salmonella* cells were directly inoculated as colonies into soft tryptone agar containing 0.35% (w/v) agar and incubated at 303 K.

2.3. Preparation of the whole-cell and culture-supernatant fractions and immunoblotting

Salmonella MKM50 ($\Delta flhB$ strain) cells (Fraser *et al.*, 2003) carrying an appropriate plasmid were incubated at 310 K in LB medium containing 100 μg ml⁻¹ ampicillin until the optical density OD₆₀₀ reached 1.4–1.5. Aliquots of culture containing a constant amount of cells were centrifuged. Cell pellets were

suspended in an equal volume of SDS loading buffer. Proteins in the culture supernatant were precipitated using 10% trichloroacetic acid and were suspended in SDS loading buffer. After SDS-PAGE, proteins were detected with anti-FlgE and anti-FliC antibodies using a WesternBreeze chromogenic immunodetection kit (Invitrogen).

2.4. Molecular-dynamics simulations

Molecular-dynamics (MD) simulations were performed using the *SCUBA* (*Simulation Codes for hUge Biomolecular Assembly*) program package (Ishida *et al.*, 2006). The AMBER ff99SB force field (Hornak *et al.*, 2006) was used for the protein. The simulated systems were solvated with SPC/E water molecules (Berendsen *et al.*, 1987) with 100 mM KCl in the periodic boundary separated by at least 12 Å from the Flh_BC molecule in the initial stage. After energy minimization and 0.27 ns MD simulation to adjust the temperature and pressure of the system to 300 K and 101 kPa with positional restraints, 40 ns MD simulation was performed without restraints in the canonical ensemble. The last 20 ns trajectory was used for the analysis. A shifted-force cutoff of real-space nonbonded energy was made at 12 Å and the particle-particle-mesh (PPPM) method (Deserno & Holm, 1998) was employed for electrostatic energy calculation in Fourier space. Integration of the equation of motion was carried out using the multi-time-step method *XO-RESPA* (Martyna *et al.*, 1996) in the canonical ensemble. Integrations of fast (bond and angle), medium (torsion and real-space nonbonded) and slow (Fourier-space nonbonded) energy terms were performed every 0.5, 1.0 and 2.0 fs, respectively.

2.5. Accession numbers

Atomic coordinates and structure factors have been deposited in the PDB with accession codes 3b0z and 3b1s for *Salmonella* and *Aquifex* Flh_BC, respectively. The structures reported here are explained in interactive three dimensions at <http://proteopedia.org/w/Samatey>.

3. Results and discussion

3.1. Flagellar Flh_BC structure description

The *Salmonella* Flh_BC (SalFlh_BC) and *Aquifex* Flh_BC (AquFlh_BC) structures were solved by multiwavelength anomalous diffraction (MAD) using selenomethionine derivatives (Meshcheryakov *et al.*, 2011; Meshcheryakov & Samatey, 2011; Table 1).

The SalFlh_BC and AquFlh_BC crystals belonged to different space groups: *P*₄₂₁₂ and *C*₂, respectively. In the case of the AquFlh_BC crystal there are three protein molecules in the asymmetric unit. The three molecules in the asymmetric unit are very similar, with r.m.s.d.s on pairwise superposition in the range 0.40–0.76 Å. Each molecule consists of two polypeptide chains resulting from proteolytic cleavage after Asn263. In all molecules no electron density was observed for residues 213–231 at the N-terminus; depending on the molecule, two to six residues at the C-terminus were disordered.

In the case of SalFlh_BC the final model comprises residues 229–353 out of 219–383 in the crystallized protein, with a cleavage after Asn269. No electron density was observed for residues 219–228 and 354–383. The model of *Salmonella* Flh_BC includes two Zn²⁺ ions and two Na⁺ ions (Fig. 1*a*). All of

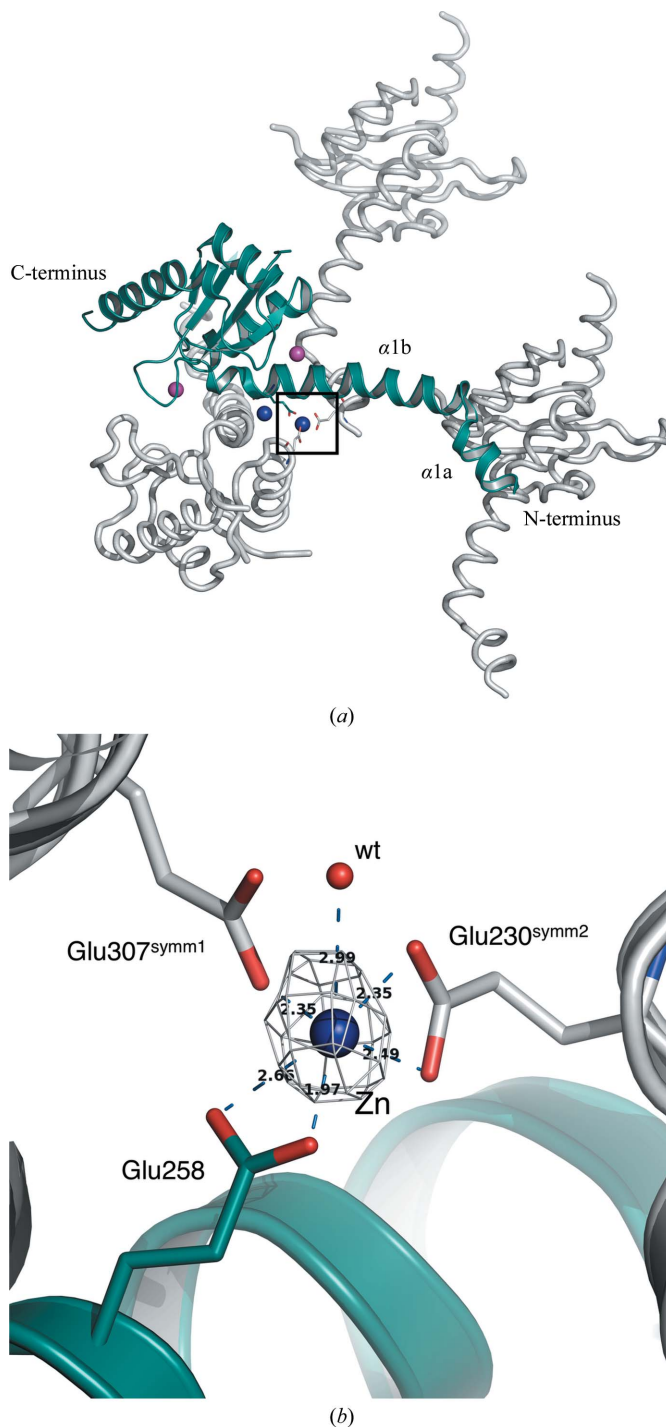
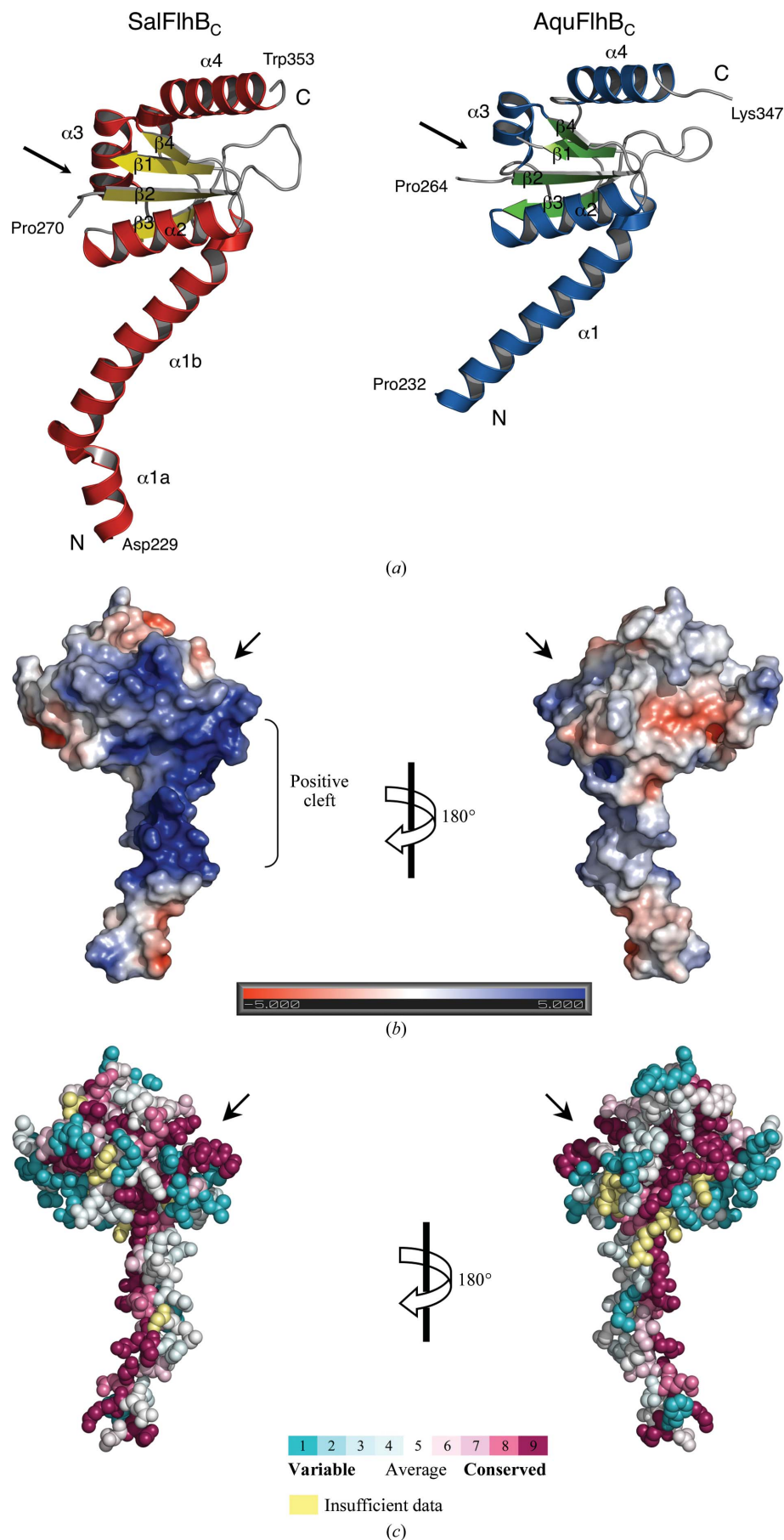


Figure 1 Molecular packing in the crystal of *Salmonella* Flh_BC. (*a*) The asymmetric molecule and symmetry-related molecules are displayed in green and grey, respectively. Sodium ions are represented as magenta spheres and zinc ions as blue spheres. (*b*) Rotated enlarged view of the zinc-binding site (black box in Fig. 1*a*). The *F_o - F_c* electron-density map is displayed in grey at a contour level of 5σ and was calculated without a Zn atom.



these atoms mediate intermolecular interactions in the crystal lattice. Zn^{2+} was added to the crystallization solution and was necessary to obtain well diffracting crystals. Analysis of the crystallographic packing shows that one of the zinc ions coordinates three symmetry-related SalFlhB_C molecules: Glu230, Glu258 and Glu307 (Fig. 1b). This interaction fixes N-terminal helix $\alpha 1$, which is one of the most flexible parts of *Salmonella* FlhB_C (see below), between two symmetrical molecules.

Both the *Salmonella* and *Aquifex* FlhB_C structures show very similar folds, with an r.m.s.d. of 1.03 Å for 102 C α atoms (Fig. 2a). Flagellar FlhB_C consists of a globular domain composed of a four-stranded β -sheet surrounded by four α -helices. The globular domain is preceded by a long N-terminal α -helix ($\alpha 1$) that connects the cytoplasmic globular part of FlhB to the transmembrane domain. The $\alpha 1$ helix engages in a crystal contact in both the *Salmonella* and *Aquifex* FlhB_C crystals, which may affect its orientation relative to the globular domain. However, these crystal contacts differ. In the SalFlhB_C crystal $\alpha 1$ primarily contacts $\alpha 1$ and $\alpha 2$ of adjacent molecules, while in the AquFlhB_C crystal $\alpha 1$ primarily contacts $\alpha 4$ and the cleavage site between $\beta 1$ and $\beta 2$.

The major difference between SalFlhB_C and AquFlhB_C is in the N-terminal region. In the model of SalFlhB_C helix $\alpha 1$ is longer and has a kink at the highly conserved residue Gly236. However, a longer helix with a kink is not excluded in AquFlhB_C, in which a highly conserved Gly230 occurs

Figure 2

Structure of flagellar FlhB_C. (a) Ribbon representation of the crystal structures of *Salmonella* and *Aquifex* FlhB_C. (b) Electrostatic potential mapped onto the surface of *Salmonella* FlhB_C. Electrostatics were calculated using the APBS software (Baker *et al.*, 2001) and plotted at $\pm 5kT e^{-1}$. (c) Evolutionarily conserved residues of FlhB_C. The figure was prepared with ConSurf (<http://consurf.tau.ac.il/>; Ashkenazy *et al.*, 2010). Residues are coloured according to the conservation in amino-acid sequences of 200 different FlhB proteins. Arrows mark the position of the autocleavage site between $\beta 1$ and $\beta 2$.

just two residues into the disordered segment 213–231 which is present in the crystallized protein but is absent in the model. Although the kink may arise from the crystal packing, our data show potential flexibility of the linker around this conserved glycine residue. The importance of such flexibility has previously been shown for EscU, an FlhB paralogue from the needle TTSS. Mutation of Gly229 (which corresponds to Gly236 of SalFlhB) to the less flexible proline in EscU completely abolished secretion (Zarivach *et al.*, 2008).

The conserved NPTH autocleavage site is exposed on a surface between strands $\beta 1$ and $\beta 2$. Both *Salmonella* and *Aquifex* FlhB_C show different conformations of the PTH region that suggest its flexibility. This is very different from the needle paralogues. In all known paralogue structures the PTH region has the same orientation, which is stabilized by contacts with surrounding residues (Zarivach *et al.*, 2008; Deane *et al.*, 2008; Wiesand *et al.*, 2009; Lountos *et al.*, 2009). It is difficult to say for the moment whether the greater flexibility of the PTH site in flagellar FlhB_C has any functional meaning. In SalFlhB_C, the PTH region, together with adjacent residues in the globular domain and the C-terminal part of the linker α -helix, forms a positively charged cleft (Fig. 2*b*). A similar positive cleft is also present in AquFlhB_C. Such a cleft might be a potential recognition site for proteins secreted by the flagellar secretion system. The autocleavage of FlhB has been suggested to create an interaction site for the other components of the type III secretion system (Zarivach *et al.*, 2008; Deane *et al.*, 2008). In particular, there is a model that describes the binding of FliK to the cleaved NPTH loop of FlhB (Mizuno *et al.*, 2011). However, the linker helix, which is one of the most conserved parts of the FlhB protein (Fig. 2*c*), could also participate in the recognition of secreted proteins, since deletions or point mutations in this region of FlhB completely block secretion (Fraser *et al.*, 2003; Zarivach *et al.*, 2008).

3.2. Comparison with needle paralogue structures

Despite low sequence identity (Fig. 3*a*), the overall structure of flagellar FlhB_C is very

similar to the structures of paralogues from the needle secretion system: EscU_C, SpaS_C, YscU_C and Spa40_C (Fig. 3*b*). The obvious difference between these proteins is the linker region between the N-terminal transmembrane domain and the globular cytoplasmic domain. All of the proteins show a large difference in the conformation of their N-terminal parts, indicating flexibility of this region of the molecule. In our structures no electron density was observed for residues 219–228 of SalFlhB_C and residues 213–231 of AquFlhB_C, which is consistent with flexibility of this part of FlhB_C. However, the remainder of the residues of the linker form a well defined α -helix, which in the case of SalFlhB_C is kinked at position Gly236. In contrast to the needle paralogues, it might be a general property of flagellar FlhB to have a more stable linker helix.

The proteins of the FlhB family exhibit a significant variation in length, mainly because of differences at the C-terminus. For instance, *Salmonella* FlhB is longer than the *Aquifex* protein by 33 amino acids. However, these additional residues

Table 2

Structure and fluctuation differences between wild-type *Salmonella* FlhB_C and its mutants during MD simulation shown by the key distance and angles defined by vectors V1–5 shown in Fig. 4(*a*).

D, length of V5. θ_{12} , θ_{23} , θ_{34} and θ_{14} , angles defined between V1 and V2, V2 and V3, V3 and V4, and V1 and V4, respectively. χ_3 and χ_5 , torsion angles defined by the sets of three vectors V2–V3–V4 (torsion around V3) and V1–V5–V4 (around V5), respectively. Averages and standard deviations over the last 20 ns of MD are shown, with negative values shown in bold.

Protein	<i>D</i> (Å)	θ_{12} (°)	θ_{23} (°)	θ_{34} (°)	θ_{14} (°)	χ_3 (°)	χ_5 (°)
<i>Salmonella</i> FlhB _C							
Wild type	37.2 ± 3.9	96.0 ± 21.9	53.8 ± 19.4	105.5 ± 2.2	77.1 ± 38.3	83.8 ± 23.5	−103.8 ± 44.8
Δ(281–285)	36.9 ± 0.7	133.2 ± 11.7	64.1 ± 5.2	108.2 ± 1.7	34.0 ± 9.5	−23.1 ± 7.9	168.3 ± 21.0
AAAAA _{281–285}	38.1 ± 1.5	113.3 ± 34.6	45.7 ± 6.1	113.2 ± 1.8	47.9 ± 35.4	30.3 ± 11.6	−175.5 ± 43.6
PPPPP _{281–285}	36.6 ± 3.1	69.6 ± 37.1	51.4 ± 12.2	112.9 ± 2.4	59.2 ± 26.9	−77.3 ± 18.9	−165.4 ± 43.1

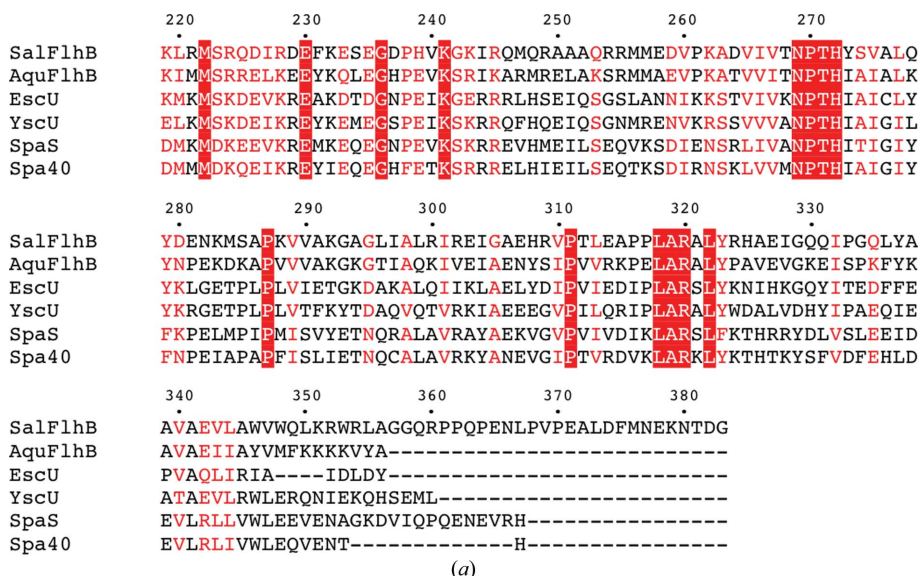


Figure 3

Comparison of flagellar FlhB_C and its paralogues from the needle type III secretion system. (*a*) Multiple sequence alignment of FlhB_C from *S. typhimurium* (SalFlhB_C; Swiss-Prot accession No. P40727) with FlhB_C from *A. aeolicus* (AquFlhB_C; O67813), EscU_C from *E. coli* (Q7DB59), YscU_C from *Yersinia pestis* (P69986), SpaS_C from *S. typhimurium* (P40702) and Spa40_C from *Shigella flexneri* (Q6XVW1). Identical residues are boxed in red; similar residues are coloured red. Alignment was performed with *ClustalW* (Larkin *et al.*, 2007; Goujon *et al.*, 2010).

(residues 354–383) were not visible in the electron-density map, suggesting that they are unfolded. This region in SalFlhB is rich in proline residues, making it unlikely to form any stable

structure. The function of the elongated C-terminal part of FlhB is not known, but it is dispensable for motility (Kutsukake *et al.*, 1994). It apparently participates in the regulation of secretion because C-terminal truncation of *Salmonella* FlhB can partially suppress the $\Delta fliK$ phenotype (Kutsukake *et al.*, 1994; Williams *et al.*, 1996). However, it is unlikely to directly interact with FliK since the truncation has almost no effect in a wild-type *fliK* background (Williams *et al.*, 1996).

3.3. Effect of mutations of residues 281–285 of *Salmonella* FlhB on TTSS function

The two strands $\beta 2$ and $\beta 3$ are connected by a long flexible loop. This loop is not conserved within the FlhB family, although it is flanked by highly conserved residues: Tyr279 and Pro287 (in *Salmonella* numbering). The length of the loop, which is longer than necessary just to connect two β -strands, made us think that it might be of functional importance. To investigate this hypothesis, we created three mutants of *Salmonella* FlhB. In the first mutant the loop residues 281–285 were deleted (Fig. 4a). In the second and third mutants residues 281–285 were substituted by Ala or Pro residues, respectively. We then carried out swarming assays on soft agar plates to investigate whether the *Salmonella* cells containing mutated FlhB were still motile. We found that the deletion of the loop completely abolished motility (Fig. 4b). At the same time, substitution by Ala residues had no effect on motility and Pro substitution decreased motility. To check whether these changes in motility were because of changes in export activity, we analyzed secretion of the hook protein FlgE and the filament protein FliC by the flagellar secretion system containing mutated FlhB (Fig. 4c). We found that motility is correlated to the secretion of FlgE and FliC. In the case in which the loop (281–285) of FlhB was deleted neither FlgE nor FliC were secreted, whereas proline substitution reduced the secretion of both proteins. No difference in secretion was observed between the wild-type FlhB and the Ala substitution.

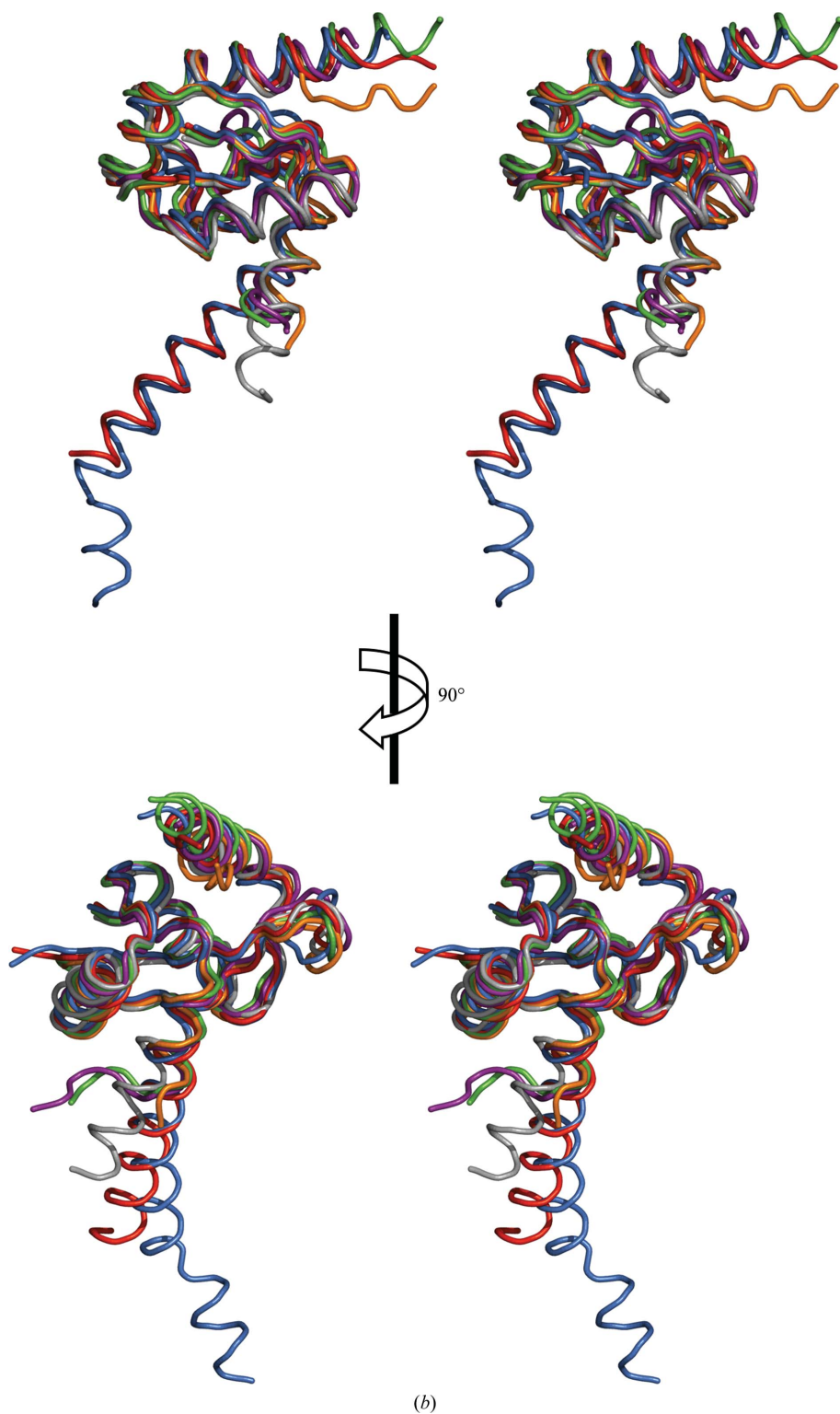
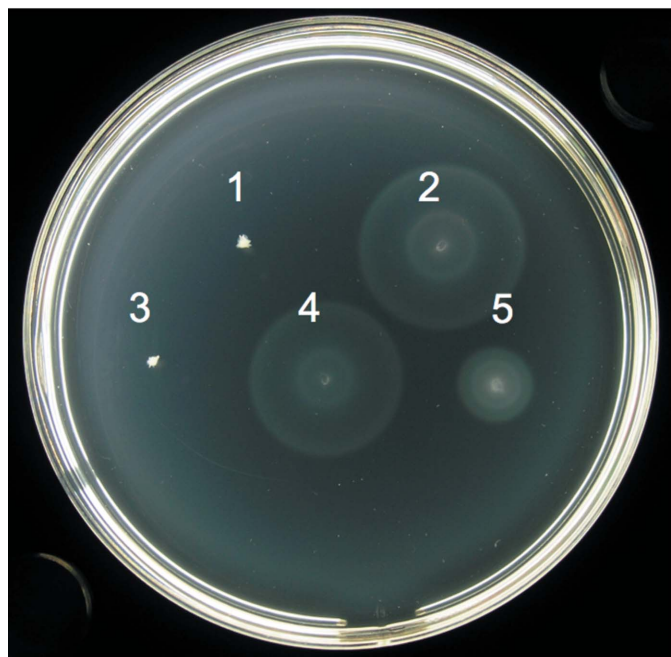
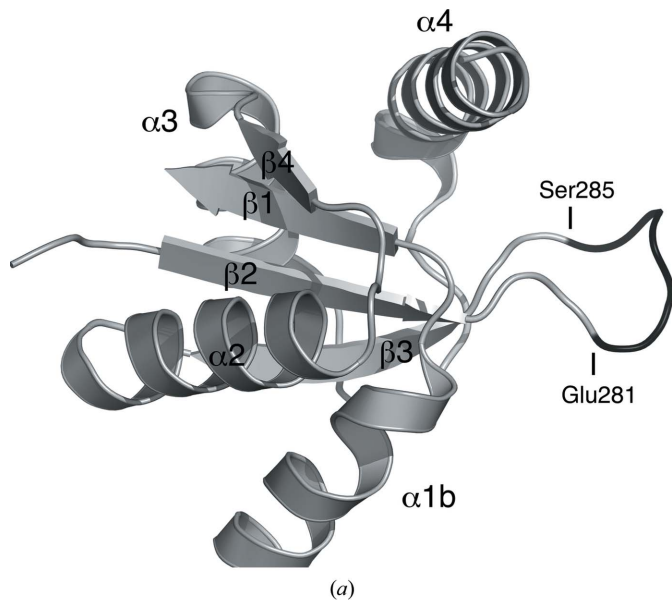


Figure 3 (continued)

(b) Stereoviews of the superposition of *Salmonella* FlhB_C (blue; PDB entry 3b0z; this work), *Aquifex* FlhB_C (red; PDB entry 3b1s; this work), EscU_C (orange; PDB entry 3bzo; Zarivach *et al.*, 2008), YscU_C (grey; PDB entry 2jli; Lountos *et al.*, 2009), SpaS_C (green; PDB entry 3c01; Zarivach *et al.*, 2008) and Spa40_C (purple; PDB entry 2vt1; Deane *et al.*, 2008).

3.4. Molecular-dynamics (MD) simulations

To further investigate the effect of mutation of the loop on the FlhB_C molecule, we performed MD simulations of the wild-type SalFlhB_C and the $\Delta(281-285)$, AAAAA₂₈₁₋₂₈₅ and PPPPP₂₈₁₋₂₈₅ mutants. During the MD simulations, we observed that the globular domain is relatively rigid in all of the cases, while the N-terminal α -helix of the wild-type FlhB_C is very flexible and becomes less flexible in the mutants (Figs. 5*b*–5*e*). In addition to the kink around Gly236–Pro238 (Fig. 2*a*), a significant kink was observed near Met256 during



the MD simulations. To characterize the flexibility of the N-terminal α -helix, we defined a distance D , angles θ_{12} , θ_{23} , θ_{34} and θ_{14} and torsion angles χ_3 and χ_5 (see explanations in Fig. 5*a* and Table 2). A notable structural difference is demonstrated by torsion angle χ_3 , which determines the direction of the V2 region of the N-terminal α -helix relative to the globular domain. The χ_3 value is positive for wild-type FlhB_C and the AAAAA₂₈₁₋₂₈₅ mutant, but is negative for the $\Delta(281-285)$ and PPPPP₂₈₁₋₂₈₅ mutants, which is consistent with the structural differences shown in Figs. 5(*b*)–5(*e*). Since the latter mutations reduce *Salmonella* motility, this structural change might have some functional effects. Another notable difference is observed as a reduction in the θ_{12} , θ_{23} , θ_{14} , χ_3 and χ_5 fluctuations in the PPPPP₂₈₁₋₂₈₅ mutant, indicating significant structural change and loss of flexibility of the N-terminal α -helix.

4. Conclusions

The flagellar secretion system is closely related to the needle type III secretion system utilized by a number of virulent bacteria for the secretion of toxins into the host-cell cytoplasm. The structure of flagellar FlhB_C described in this paper once again confirms this relationship. Basically, the structure is similar to already known structures of needle paralogues. The differences (such as the orientation of the conserved PTH sequence or the longer linker helix) could be peculiarities of the flagellar protein. The functional implications of such differences, if any, are a subject for further investigation.

The most important of our findings is that flexibility of the large nonconserved loop in the globular domain of FlhB_C is

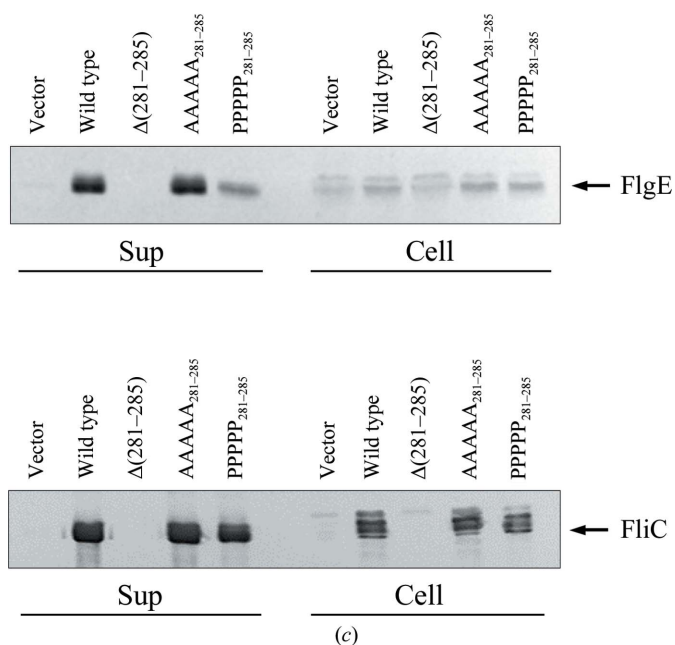


Figure 4

Effect of mutations of the ENKMS₂₈₁₋₂₈₅ region of *Salmonella* FlhB on protein function. (a) Ribbon representation of *Salmonella* FlhB_C; the region is shown in black. (b) The ability of FlhB variants with a modified ENKMS region to complement the $\Delta flhB$ *Salmonella* strain MKM50. Motility assays were carried out on semi-solid agar plates at 303 K for 5 h. FlhB products were 1, none, empty vector; 2, wild-type FlhB; 3, FlhB $\Delta(281-285)$; 4, FlhB AAAAA₂₈₁₋₂₈₅; 5, FlhB PPPPP₂₈₁₋₂₈₅. (c) Immunoblotting using anti-FlgE and anti-FliC antibodies on the whole-cell (Cell) and culture-supernatant (Sup) fractions from *Salmonella* strain MKM50 producing different FlhB variants.

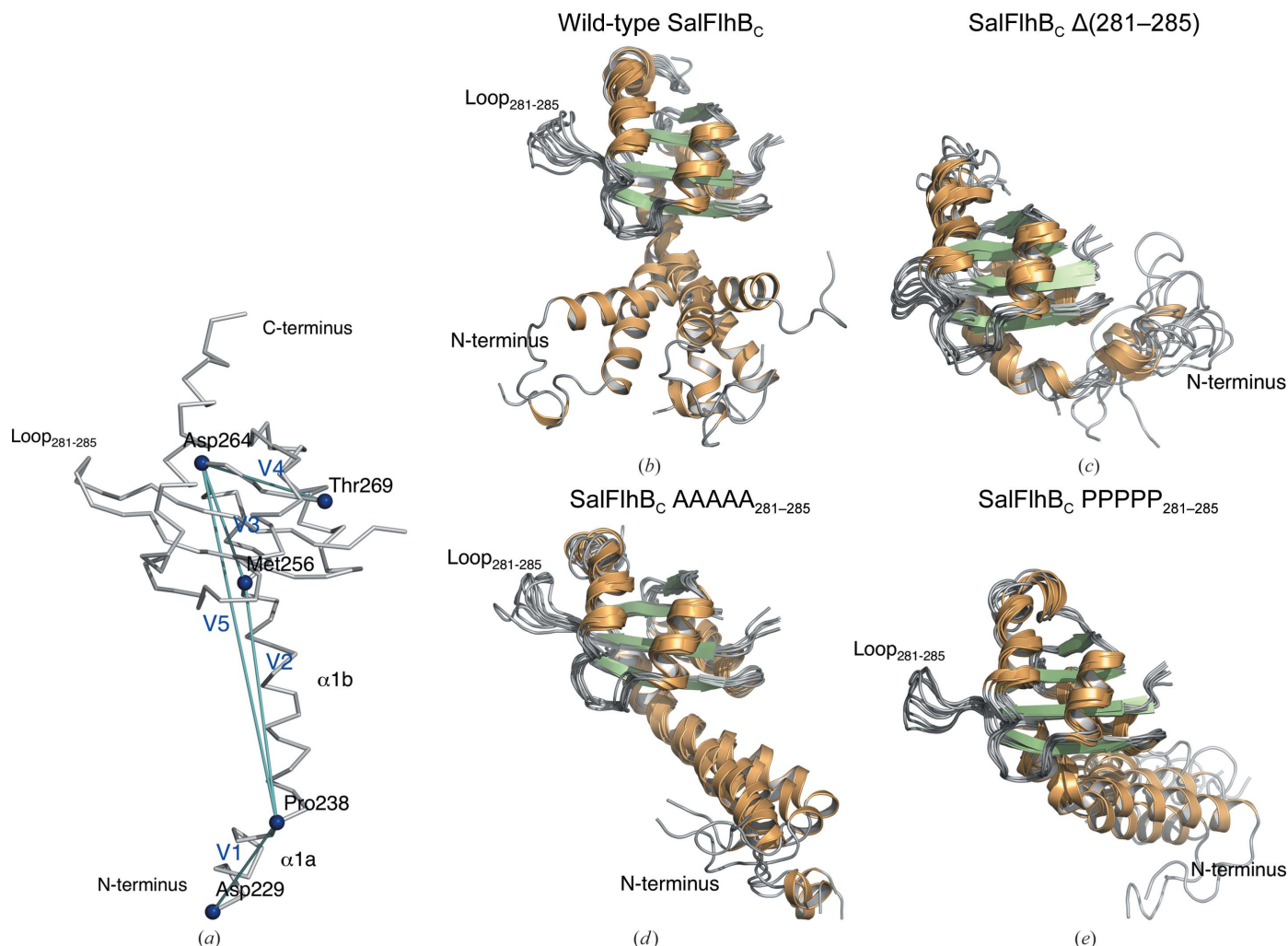


Figure 5

Flexibility of the N-terminal α -helix of *Salmonella* FlhB_C observed in MD simulations. (a) Key residues and vectors used for MD analysis in Table 2. The vectors connecting residues 229–238, 238–256, 256–264, 265–269 and 238–264 are defined as V1–V5, respectively. (b–e) Structural variations of the N-terminal α -helix during MD simulations when the globular domain is superimposed for (b) the wild-type FlhB_C, (c) FlhB_C Δ (281–285), (d) FlhB_C AAAAA_{281–285} and (e) FlhB_C PPPPP_{281–285}. For each case, six snapshots were chosen based on the maximum and minimum values of D , θ_{14} and χ_5 (see Table 2 for their definitions).

necessary for function of the whole secretion system. Deletion of this loop or its mutation to less flexible proline residues makes FlhB_C more rigid and thus abolishes or significantly reduces secretion. Taking into account the similarity between the flagellar and needle proteins, this loop could be a promising target for the creation of novel drugs against pathogenic bacteria.

We thank Y.-H. Yoon and I. Meshcheryakova for help with the experiments. We thank the staff at beamlines BL44XU and BL41XU at the SPring-8 synchrotron, Harima, Japan for support in obtaining beam time and assistance with X-ray data collection. We are grateful to the School of Frontier Biosciences, Osaka University for the *Salmonella* strains. We thank E. Martz at the University of Massachusetts, Amherst, USA for making the Proteopedia web pages and the videos. This work was supported by direct funding provided by OIST. Computations were performed using the computers at OIST, IMCB/University of Tokyo, the Research Center for

Computational Science/Okazaki Research Facilities/National Institute of Natural Science and the Institute for Solid State Physics/University of Tokyo.

References

- Aizawa, S.-I. (2001). *FEMS Microbiol. Lett.* **202**, 157–164.
- Ashkenazy, H., Erez, E., Martz, E., Pupko, T. & Ben-Tal, N. (2010). *Nucleic Acids Res.* **38**, W529–W533.
- Baker, N. A., Sept, D., Joseph, S., Holst, M. J. & McCammon, J. A. (2001). *Proc. Natl Acad. Sci. USA*, **98**, 10037–10041.
- Berendsen, H. J. C., Grigera, J. R. & Straatsma, T. P. (1987). *J. Phys. Chem.* **91**, 6269–6271.
- Blocker, A., Komoriya, K. & Aizawa, S. (2003). *Proc. Natl Acad. Sci. USA*, **100**, 3027–3030.
- Cowtan, K. (2006). *Acta Cryst.* **D62**, 1002–1011.
- Deane, J. E., Graham, S. C., Mitchell, E. P., Flot, D., Johnson, S. & Lea, S. M. (2008). *Mol. Microbiol.* **69**, 267–276.
- Deserno, M. & Holm, C. (1998). *J. Chem. Phys.* **109**, 7678.
- Emsley, P., Lohkamp, B., Scott, W. G. & Cowtan, K. (2010). *Acta Cryst.* **D66**, 486–501.

- Ferris, H. U., Furukawa, Y., Minamino, T., Kroetz, M. B., Kihara, M., Namba, K. & Macnab, R. M. (2005). *J. Biol. Chem.* **280**, 41236–41242.
- Ferris, H. U. & Minamino, T. (2006). *Trends Microbiol.* **14**, 519–526.
- Fraser, G. M., Hirano, T., Ferris, H. U., Devgan, L. L., Kihara, M. & Macnab, R. M. (2003). *Mol. Microbiol.* **48**, 1043–1057.
- Goujon, M., McWilliam, H., Li, W., Valentin, F., Squizzato, S., Paern, J. & Lopez, R. (2010). *Nucleic Acids Res.* **38**, W695–W699.
- Hirano, T., Minamino, T., Namba, K. & Macnab, R. M. (2003). *J. Bacteriol.* **185**, 2485–2492.
- Hirano, T., Yamaguchi, S., Oosawa, K. & Aizawa, S. (1994). *J. Bacteriol.* **176**, 5439–5449.
- Hornak, V., Abel, R., Okur, A., Strockbine, B., Roitberg, A. & Simmerling, C. (2006). *Proteins*, **65**, 712–725.
- Ishida, H., Higuchi, M., Yonetani, Y., Kano, T., Joti, Y., Kitao, A. & Go, N. (2006). *Annual Report of the Earth Simulator Center*, pp. 237–239. Yokohama: Earth Simulator Center, Japan Agency for Marine-Earth Science and Technology.
- Kutsukake, K., Minamino, T. & Yokoseki, T. (1994). *J. Bacteriol.* **176**, 7625–7629.
- Larkin, M. A., Blackshields, G., Brown, N. P., Chenna, R., McGettigan, P. A., McWilliam, H., Valentin, F., Wallace, I. M., Wilm, A., Lopez, R., Thompson, J. D., Gibson, T. J. & Higgins, D. G. (2007). *Bioinformatics*, **23**, 2947–2948.
- Lountos, G. T., Austin, B. P., Nallamsetty, S. & Waugh, D. S. (2009). *Protein Sci.* **18**, 467–474.
- Martyna, G. J., Tuckerman, M. E., Tobias, D. J. & Klein, M. L. (1996). *Mol. Phys.* **87**, 1117–1157.
- Meshcheryakov, V. A. & Samatey, F. A. (2011). *Acta Cryst.* **F67**, 808–811.
- Meshcheryakov, V. A., Yoon, Y.-H. & Samatey, F. A. (2011). *Acta Cryst.* **F67**, 280–282.
- Minamino, T., Iino, T. & Kutuskake, K. (1994). *J. Bacteriol.* **176**, 7630–7637.
- Minamino, T. & Macnab, R. M. (1999). *J. Bacteriol.* **181**, 1388–1394.
- Minamino, T. & Macnab, R. M. (2000a). *J. Bacteriol.* **182**, 4906–4914.
- Minamino, T. & Macnab, R. M. (2000b). *Mol. Microbiol.* **35**, 1052–1064.
- Minamino, T., Saijo-Hamano, Y., Furukawa, Y., González-Pedrajo, B., Macnab, R. M. & Namba, K. (2004). *J. Mol. Biol.* **341**, 491–502.
- Mizuno, S., Amida, H., Kobayashi, N., Aizawa, S. & Tate, S. (2011). *J. Mol. Biol.* **409**, 558–573.
- Morris, D. P., Roush, E. D., Thompson, J. W., Moseley, M. A., Murphy, J. W. & McMurry, J. L. (2010). *Biochemistry*, **49**, 6386–6393.
- Murshudov, G. N., Skubák, P., Lebedev, A. A., Pannu, N. S., Steiner, R. A., Nicholls, R. A., Winn, M. D., Long, F. & Vagin, A. A. (2011). *Acta Cryst.* **D67**, 355–367.
- Painter, J. & Merritt, E. A. (2006). *Acta Cryst.* **D62**, 439–450.
- Sheldrick, G. M. (2008). *Acta Cryst.* **A64**, 112–122.
- Wang, W. & Malcolm, B. A. (1999). *Biotechniques*, **26**, 680–682.
- Wiesand, U., Sorg, I., Amstutz, M., Wagner, S., van den Heuvel, J., Lührs, T., Cornelis, G. R. & Heinz, D. W. (2009). *J. Mol. Biol.* **385**, 854–866.
- Williams, A. W., Yamaguchi, S., Togashi, F., Aizawa, S.-I., Kawagishi, I. & Macnab, R. M. (1996). *J. Bacteriol.* **178**, 2960–2970.
- Winn, M. D. *et al.* (2011). *Acta Cryst.* **D67**, 235–242.
- Zarivach, R., Deng, W., Vuckovic, M., Felise, H. B., Nguyen, H. V., Miller, S. I., Finlay, B. B. & Strynadka, N. C. (2008). *Nature (London)*, **453**, 124–127.
- Zhu, K., González-Pedrajo, B. & Macnab, R. M. (2002). *Biochemistry*, **41**, 9516–9524.